

# Reactions of the CN Radical with Benzene and Toluene: Product Detection and Low-Temperature Kinetics

Adam J. Trevitt,<sup>\*,†,§</sup> Fabien Goulay,<sup>‡</sup> Craig A. Taatjes,<sup>‡</sup> David L. Osborn,<sup>‡</sup> and Stephen R. Leone<sup>\*,†,#</sup>

Departments of Chemistry and Physics, and Lawrence Berkeley National Laboratory, University of California, Berkeley, California 94720, and Combustion Research Facility, Mail Stop 9055, Sandia National Laboratories, Livermore, California, Livermore, California 94551-0969

Received: October 8, 2009; Revised Manuscript Received: December 3, 2009

Low-temperature rate coefficients are measured for the CN + benzene and CN + toluene reactions using the pulsed Laval nozzle expansion technique coupled with laser-induced fluorescence detection. The CN + benzene reaction rate coefficient at 105, 165, and 295 K is found to be relatively constant over this temperature range,  $(3.9\text{--}4.9) \times 10^{-10} \text{ cm}^3 \text{ molecule}^{-1} \text{ s}^{-1}$ . These rapid kinetics, along with the observed negligible temperature dependence, are consistent with a barrierless reaction entrance channel and reaction efficiencies approaching unity. The CN + toluene reaction is measured to have a rate coefficient of  $1.3 \times 10^{-10} \text{ cm}^3 \text{ molecule}^{-1} \text{ s}^{-1}$  at 105 K. At room temperature, nonexponential decay profiles are observed for this reaction that may suggest significant back-dissociation of intermediate complexes. In separate experiments, the products of these reactions are probed at room temperature using synchrotron VUV photoionization mass spectrometry. For CN + benzene, cyanobenzene ( $\text{C}_6\text{H}_5\text{CN}$ ) is the only product recorded with no detectable evidence for a  $\text{C}_6\text{H}_5 + \text{HCN}$  product channel. In the case of CN + toluene, cyanotoluene ( $\text{NCC}_6\text{H}_4\text{CH}_3$ ) constitutes the only detected product. It is not possible to differentiate among the ortho, meta, and para isomers of cyanotoluene because of their similar ionization energies and the  $\sim 40 \text{ meV}$  photon energy resolution of the experiment. There is no significant detection of benzyl radicals ( $\text{C}_6\text{H}_5\text{CH}_2$ ) that would suggest a H-abstraction or a HCN elimination channel is prominent at these conditions. As both reactions are measured to be rapid at 105 K, appearing to have barrierless entrance channels, it follows that they will proceed efficiently at the temperatures of Saturn's moon Titan ( $\sim 100 \text{ K}$ ) and are also likely to proceed at the temperature of interstellar clouds ( $10\text{--}20 \text{ K}$ ).

## 1. Introduction

Significant interest surrounds the reactions of CN radicals with hydrocarbons in the context of planetary atmospheres, interstellar media, and combustion, particularly concerning the gas-phase product pathways leading to nitrile alkenes, polyaromatic hydrocarbon (PAH) nitriles, and polyaromatic nitrogen heterocyclics (PANHs). The chemistry—formation and fate—of CN-bearing molecules in the atmosphere of Saturn's moon Titan is one example where these reactions are thought to be integral.<sup>1,2</sup> The hazy atmosphere of Titan presents a fascinating chemical system for which experimental data from the Cassini mission continues to be collected and interpreted. Mass spectra gathered from the ion neutral mass spectrometer (INMS) on board Cassini reveal the presence of, and in some cases quantify, numerous neutral hydrocarbons (including  $\text{C}_2\text{H}_2$ ,  $\text{C}_2\text{H}_4$ ,  $\text{CH}_3\text{C}_2\text{H}$ , and  $\text{C}_4\text{H}_2$ ) and nitrogen-bearing species (e.g.,  $\text{HC}_3\text{N}$ ,  $\text{C}_2\text{N}_2$ , and  $\text{NH}_3$ ).<sup>3</sup>

Benzene ( $\text{C}_6\text{H}_6$ ) is also identified in the Titan atmosphere by the INMS.<sup>4,5</sup> Further verification of the presence of benzene in the atmosphere is reported by Coustenis et al. utilizing data acquired from the composite infrared spectrometer on board

Cassini.<sup>6</sup> The Huygens lander probe, launched from Cassini, may have also detected evidence for benzene residing on Titan's surface using its onboard gas chromatograph mass spectrometer.<sup>7</sup> A mass consistent with  $\text{C}_7\text{H}_8$  (toluene) is also recorded by the INMS, but it has been suggested that quantification of toluene is affected by possible wall-mediated chemistry within the sampling portion of the INMS that leads to products at the toluene mass.<sup>3,8</sup> The  $\text{C}_6\text{H}_5 + \text{CH}_3$  reaction is a plausible neutral radical–radical pathway leading to the formation of toluene in Titan's atmosphere.<sup>8</sup> Complex molecules with masses up to 350 Da along with negative ions with masses up to  $\sim 8000 \text{ Da}$  have been detected.<sup>5</sup> It is proposed that these large molecules and ions, which are postulated to be unsaturated hydrocarbons including PAH and PANH compounds, are the precursors that condense to form particulate matter.<sup>5</sup> Generally, benzene is considered pivotal in the formation of PAHs that in turn lead to the growth of particles/aerosol that are responsible for Titan's hazy appearance.<sup>5</sup> A recent study proposes sequential  $\text{C}_2\text{H}$  radical addition reactions starting with benzene as a PAH growth mechanism.<sup>9</sup> This centrality of benzene in the molecular weight growth schemes is not confined to the context of Titan haze formation; it is also commonly accepted that benzene is integral to the formation of carbonaceous soot particles in combustion environments.<sup>10</sup> Schemes leading to PAH formation are emerging, but the key neutral reactions that incorporate nitrogen into the molecular weight growth chemistry, most likely implicating  $\text{—CN}$  species and yielding PANH scaffolds, remain unclear.

\* To whom correspondence should be addressed. E-mail: adamt@uow.edu.au (A.J.T.); srl@berkeley.edu (S.R.L.).

<sup>†</sup> University of California, Berkeley.

<sup>‡</sup> Sandia National Laboratories.

<sup>§</sup> Present address: School of Chemistry, University of Wollongong, Wollongong, NSW, 2522, Australia.

<sup>#</sup> On appointment as a Miller Research Professor in the Miller Institute for Basic Research in Science.

A particularly salient physical parameter when considering Titan's atmospheric chemistry is its low temperature (100–200 K). Predicting and modeling the evolution of Titan's atmosphere requires chemical data in the form of rate coefficients and reaction product branching ratios. Detailed low-temperature product branching fractions are particularly scant. Low-temperature rate coefficients for radical–neutral reactions, on the other hand, have been accumulating in recent years primarily due to the efforts of the groups at Rennes, Birmingham, and Berkeley using Laval nozzle expansion techniques. Many of these reactions have been recently reviewed.<sup>11</sup> It is now known that extrapolating kinetic data acquired at moderate temperatures (300–1000 K) down to very low temperatures (<300 K) can yield rate coefficients that disagree with measured data by as much as several orders of magnitude. The measurement of rate coefficients at the relevant low temperatures is therefore vital for accurate kinetic data. Recently, low-temperature kinetic studies have been extended to aromatic species: benzene<sup>12–14</sup> and anthracene.<sup>15,16</sup>

The low-temperature reactivity of the CN radical has been investigated for a range of small hydrocarbons.<sup>17</sup> The reactions of CN with larger hydrocarbon species including allene and propyne were found to have rate coefficients of  $\sim 4 \times 10^{-10}$  cm<sup>3</sup> molecule<sup>-1</sup> s<sup>-1</sup> over the 15–294 K range.<sup>18</sup> Bimolecular rates of this value are approaching the gas-kinetic limit. Reactions of CN with unsaturated hydrocarbons that have near-collision-limited rate coefficients at room temperature represent examples where the kinetics depends predominantly on long-range capture processes (i.e., are barrierless reactions) such that it is likely the reaction rate will remain rapid down to much lower temperatures. This notion has yet to be tested for CN reactions with aromatic species. A rate coefficient for the CN + benzene reaction has been determined only at room temperature to be  $2.8 \times 10^{-10}$  cm<sup>3</sup> molecule<sup>-1</sup> s<sup>-1</sup>.<sup>19</sup> To our knowledge, no kinetic data have been reported for the CN + toluene reaction at any temperature.

Crossed molecular beam studies comprise a significant portion of the product detection studies concerned with CN + hydrocarbon reactions.<sup>20,21</sup> Balucani et al. investigated the CN + benzene reaction at collision energies between 19.5 and 34.4 kJ/mol and compared the results to electronic structure and RRKM calculations.<sup>22</sup> It was concluded that the dominant reaction entrance channel is barrierless leading to the formation of a CN-addition complex (C<sub>6</sub>H<sub>6</sub>CN) that subsequently dissociates to form cyanobenzene (C<sub>6</sub>H<sub>5</sub>CN) + H. The isocyanobenzene (C<sub>6</sub>H<sub>5</sub>NC) product channel was set to a limit of less than 2%. To our knowledge, there has not been a similar study concerned with the CN + toluene reaction.

Recently, we reported on the room temperature reactions of CN + ethene and CN + propene reactions utilizing synchrotron VUV multiplexed photoionization mass spectrometry (MPIMS).<sup>23</sup> Product species were identified using adiabatic ionization energies (AIEs) and characteristic photoionization efficiency (PIE) curves. These data were analyzed with either known or approximated photoionization cross sections to ultimately assign product branching fractions.

In this paper, we report the low-temperature rate coefficients measured for the CN + benzene (105–295 K) and the CN + toluene (105 K) reactions conducted using a pulsed Laval nozzle expansion coupled with laser-induced fluorescence detection. We also report product detection experiments for both reactions conducted at room temperature using synchrotron MPIMS to elucidate the dominant reaction products of these reactions.

## 2. Experimental Section

The low-temperature kinetic data are obtained using a pulsed Laval nozzle expansion, using several nozzles designed to work at different temperatures. Laser photolysis is employed for the production of CN radicals and the relative concentration of these radicals are subsequently tracked using laser-induced fluorescence (LIF). The experimental arrangement and characterization of the Laval nozzle apparatus used in this work are described in detail in previous papers,<sup>12,24</sup> so just a brief overview of the experiment is given herein.

A pulse of gas mixture, containing mostly N<sub>2</sub> with traces of CN radical precursor (cyanogen iodide, ICN) and aromatic hydrocarbon (benzene or toluene), is expanded through a Laval nozzle into the reaction vacuum chamber. The notable feature of the Laval expansion is that, under optimal operating conditions, a collimated supersonic gas flow is established for approximately 15 cm into the reaction chamber. This collimated flow has uniform temperature and density distributions in both the radial and axial directions. In a sense, the Laval expansion can be thought of as a wall-less flow tube where reactions can be studied at very low temperatures without the complicating effects of wall condensation. Nozzles are fabricated to produce a collimated flow with a particular temperature that depends on the nozzle geometry, the buffer gas, and the temperature of the gas entering the nozzle. These nozzles are designed to be interchangeable in order to perform kinetic measurements at various temperatures. The nozzles used in this work generate flows of 105 K (Mach 3) and 165 K (Mach 2). The pressure in the reaction chamber is adjusted using N<sub>2</sub> gas in order to obtain optimal collimation in the Laval gas flow. Four milliseconds after the initiation of the gas pulse, an  $\sim 7$  ns 40 mJ/cm<sup>2</sup> laser pulse (266 nm, fourth harmonic of Nd:YAG), unfocused, is directed down the central bore of the Laval flow. This pulse generates CN radicals from the photolysis of ICN with the initial radical concentration estimated to be  $\sim 1 \times 10^{10}$  molecules/cm<sup>3</sup>. The concentration of CN radicals is monitored via LIF. To accomplish this task, a second pulsed Nd:YAG laser operating on the third harmonic (355 nm) pumps a dye laser (using Exalite 392A dye in *p*-dioxane) that is tuned to excite CN radicals on the R(4) line of the (0,0) B<sup>2</sup>Σ<sup>+</sup>–X<sup>2</sup>Σ<sup>+</sup> system at  $\sim 387$  nm coaxially down the Laval expansion. Fluorescence is detected perpendicular to the excitation axis, 12 cm downstream of the Laval nozzle by a photomultiplier tube through a 10 nm wavelength bandpass filter centered at 420 nm corresponding to the (0,1) B<sup>2</sup>Σ<sup>+</sup>–X<sup>2</sup>Σ<sup>+</sup> band. The photomultiplier signal is processed in analog fashion using a box-car integrator set to a delay so that there was minimal interference from the LIF probe laser beam in the integrated CN LIF signal. Measuring the CN LIF as a function of delay between the photolysis laser and the LIF probe laser permits the CN radical concentration to be followed as a function of reaction time. Typically, 10 laser pulses are averaged per point with 5–10 decay profiles subsequently summed together for pseudo-first-order kinetic analysis. The experiment is performed at a 10 Hz repetition rate.

All gas flows are controlled using calibrated mass-flow controllers. The aromatic reactant, benzene (purity >99.5%) or toluene (purity >99.8%), is entrained in the gas flow by bubbling a fixed flow of nitrogen (15 sccm) through a liquid sample of either benzene or toluene. The concentration of the aromatic reactant is varied by changing the pressure in the bubbler using the needle valve on the output side of the bubbler. The temperature of the bubbler was maintained below room temperature, typically at 15 °C, using a water bath chiller. Varying the bubbler reservoir temperature showed no measurable change

in the kinetic measurements over 10–20 °C. With knowledge of the temperature of the liquid in the bubbler and pressure above the liquid sample in the bubbler, it is possible to calculate the density of either benzene or toluene entrained in the gas flow. To ensure thorough mixing of the N<sub>2</sub> and benzene or toluene vapor, N<sub>2</sub> is supplied to the bubbler through a glass frit. After the bubbler, a mixing volume of 500 mL is in place. All tubing after the bubbler/chiller is at room temperature. The system is given ample time to equilibrate between acquisitions and this is confirmed by consecutive concordant measurements. The temperature-dependent vapor pressures for both benzene and toluene are calculated from their known Antoine parameters.<sup>25</sup>

Product detection experiments are conducted on the multiplexed photoionization mass spectrometer at the Chemical Dynamics Beamline at the Advanced Light Source, Lawrence Berkeley National Laboratory. Products of the CN + benzene and the CN + toluene reaction are measured by using tunable synchrotron VUV photoionization mass spectrometry. The experimental apparatus is described comprehensively in recent literature,<sup>26</sup> and we recently reported product detection studies of CN reacting with ethene and propene using this configuration.<sup>23</sup> Briefly, the experiment couples a reaction flow tube to a magnetic sector mass spectrometer utilizing the tunable, synchrotron VUV photons to selectively ionize neutral species. The gas in the reaction flow tube is maintained at 4 Torr, made up of the radical precursor (ICN), a known concentration of coreactant (benzene or toluene) and He buffer gas. Radical–neutral reactions are initiated by an excimer laser pulse (KrF, 248 nm) that photolyzes ICN to form CN radicals uniformly down the reaction flow tube. A portion of the gas flow in the reaction tube escapes through a 650  $\mu$ m pinhole, situated 350 mm down the flow tube, into a differentially pumped vacuum chamber. This effusive gas, containing reactants, products, and buffer gas, is sampled by a skimmer forming a molecular beam that is directed into a differentially pumped chamber. Here, the molecular beam is intersected with the VUV synchrotron photon beam and photoions are then extracted and separated according to their mass-to-charge ( $m/z$ ) ratios using a compact magnetic-sector mass spectrometer. In this configuration ions are time-tagged relative to the pulsing of the excimer laser allowing individual  $m/z$  channels to be monitored as a function of kinetic time. Reactant, intermediate and product species can then be distinguished on the basis of their temporal profiles. In an additional dimension, scanning the VUV photon energy allows the photoionization efficiency (PIE) of the  $m/z$  channels to be recorded. These PIE curves are then used to distinguish molecular isomers on the basis of their adiabatic ionization energies (AIEs) and characteristic PIE responses as described later in this report.

### 3. Results

**3.1. Low-Temperature Kinetics.** Previous low-temperature kinetic studies concerned with CN reactivity predominantly used NCNO as a CN radical precursor photolyzed by either 532 or 583 nm laser irradiation.<sup>17,27,28</sup> In the current study, the 266 nm laser photolysis of ICN is employed to generate CN radicals. To check for consistency, the kinetics of the CN + C<sub>2</sub>H<sub>4</sub> reaction was measured at 105 K and compared with data from Sims et al.<sup>17</sup> who studied the reaction kinetics over 25–295 K with NCNO as the CN radical precursor. A rate coefficient of  $3.6 \times 10^{-10}$  cm<sup>3</sup> molecule<sup>-1</sup> s<sup>-1</sup> is measured for this reaction using ICN as the CN photolysis precursor and fits well with the trend measured by Sims et al. (Figure 1). It is perhaps worth

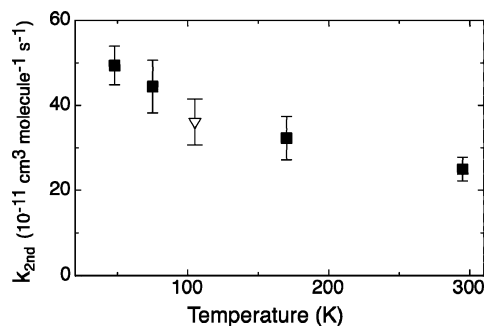


**Figure 1.** Measured CN + C<sub>2</sub>H<sub>4</sub> bimolecular rate coefficient determined in this work at 105 K using ICN as the CN radical photolysis precursor (triangle) compared to the data taken from Sims et al.<sup>17</sup> where NCNO was used as the CN photolysis precursor (squares).

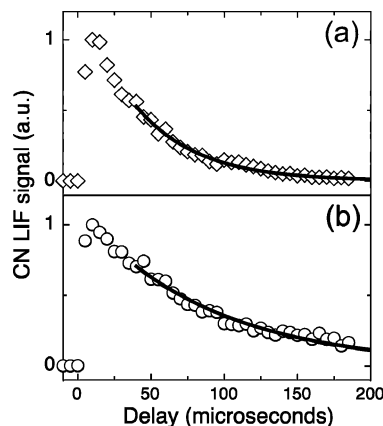


**Figure 2.** Decay profiles of the CN radical measured at 105 K for the (a) CN + benzene reaction with a benzene density of  $4.83 \times 10^{13}$  cm<sup>-3</sup> and the (b) CN + toluene reaction with a toluene density of  $4.63 \times 10^{13}$  cm<sup>-3</sup>. Both are fitted to single-exponential decays (solid line). The delay is the timing delay between the photolysis laser pulse and the laser-induced fluorescence probe laser pulse.

mentioning, due to an apparent reduced commercial availability of ICN, that BrCN (photolyzed at 248 nm) was found to be an unsuitable precursor for low-temperature CN radical kinetics studies in an N<sub>2</sub> buffer gas. Substantial rotational excitation imparted to the CN fragment was observed in measured LIF excitation spectra, as has been reported,<sup>29</sup> and thermalization was found to be relatively slow. This effect manifests itself as a reduction of the observed CN decay rates because the removal of CN via reaction is compensated to a small but measurable extent by quenching of high rotational energy levels that repopulate the low rotational state probed using the LIF scheme. In contrast, a LIF excitation spectrum acquired at a 40  $\mu$ s delay after pulsing the photolysis laser confirms that CN radicals generated from ICN photolysis are rotationally thermalized to 105 and 165 K, for the respective Laval nozzle, and the population almost entirely occupies the vibrational ground state.

Rate coefficients for the CN + benzene reaction were measured at 105, 165 and 295 K. Pseudo-first-order decay profiles (Figure 2a) were recorded over a range of benzene densities. In the case of CN + toluene, the rate coefficient for this reaction at the Titan relevant temperature of 105 K is measured to be  $1.3 \times 10^{-10}$  cm<sup>3</sup> molecule<sup>-1</sup> s<sup>-1</sup>. Nonexponential decay profiles were observed for this reaction at room temperature. A representative decay profile at 105 K is depicted in Figure 2b. For both reactions, single-exponential decay profiles are fitted for delay times >40  $\mu$ s, ensuring good thermalization of the CN radicals. Bimolecular rate coefficients are subsequently obtained from the slopes of the straight-line fit from



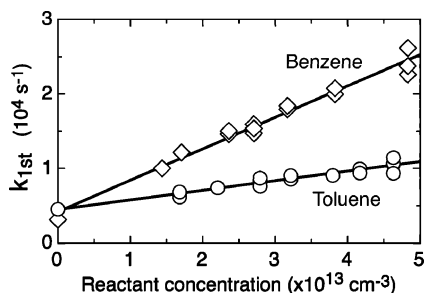


**Figure 3.** Pseudo-first-order plots measured at 105 K for the CN + benzene (diamonds) and CN + toluene (circles) reactions.

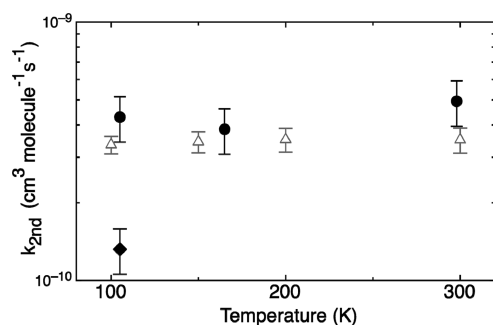


**Figure 4.** Measured bimolecular rate coefficients for the CN + benzene reaction (circles) compared with computationally predicted values from Woon<sup>31</sup> (triangles) and the CN + toluene bimolecular rate coefficient measured at 105 K (diamond).

the pseudo-first-order rate coefficients plotted as a function of benzene or toluene density (Figure 3). The nonzero pseudo-first-order rate coefficients recorded for CN radicals at zero concentration of aromatic coreactant is likely due to diffusion of CN species out of the laser photolysis/LIF region. Interference from the CN + ICN reaction is not expected to be kinetically competitive based on CN + BrCN and CN + ClCN kinetic studies that obtained rate coefficients of  $9 \times 10^{-14}$  and  $2.1 \times 10^{-13} \text{ cm}^3 \text{ molecule}^{-1} \text{ s}^{-1}$ , respectively.<sup>30</sup>

The determined rate coefficients vs temperature are presented in Figure 4 and these data, along with experimental conditions, are displayed in Table 1. Within the uncertainty of the experiment, the rate coefficient for the CN + benzene reaction remains essentially unchanged over the 105–295 K temperature range. For comparison, Figure 4 also displays data from Woon,<sup>31</sup> who investigated the kinetics of the CN + benzene reaction computationally over this temperature range.

The statistical uncertainty for the data displayed in Table 1 is  $2\sigma < 10\%$ , where  $\sigma$  is obtained from the least-squares fit to the pseudo-first-order decay profiles with each rate coefficient, measured in duplicate. Any systematic uncertainty in the rate coefficients is primarily attributed to the uncertainty in the concentration of the aromatic coreactant, which depends on the pressure over the liquid the bubbler, the temperature of the bubbler, and the flow rate of gas through the bubbler. Uncertainty in the measurements of the temperature and pressure within the bubbler affect the calculated density of aromatic vapor in the flow. In all, error bars of 20% are ascribed to the measured rate coefficients to take into account statistical and systematic uncertainties. Variation in the aromatic number density due to photofragmentation from the 266 nm laser pulse should be  $<1\%$  because the absorption cross sections for both benzene and toluene at 266 nm have been measured at  $<2 \times 10^{-19} \text{ cm}^2$ .<sup>32</sup>

**3.2. Product Detection.** The product detection experiments at the Advanced Light Source (ALS) synchrotron are performed at room temperature for the CN + benzene and CN + toluene

reactions. For CN + benzene, one product is detected from this reaction occurring at  $m/z = 103$ . Examining the PIE spectrum of this mass reveals an onset of signal at  $9.70 \pm 0.05 \text{ eV}$ . The PIE curve is compared to a photoelectron spectrum of cyanobenzene<sup>33</sup> that has been digitized and integrated over energy, revealing a good match (Figure 5). The AIE of cyanobenzene has been determined by ZEKE photoelectron spectroscopy to be  $9.7315 \text{ eV}$ .<sup>34</sup> The agreement between the onset of the ion signal in the measured PIE and the integrated photoelectron spectrum of cyanobenzene is consistent with cyanobenzene being the major product for this mass channel. The vertical IE of isocyanobenzene ( $\text{C}_6\text{H}_5\text{NC}$ ) has been measured to have a value of  $9.5 \text{ eV}$ ,<sup>35</sup> and we see no apparent onset of signal around this vicinity in the measured PIE spectrum of  $m/z = 103$ ; an estimate of  $<10\%$  branching fraction for the isocyanobenzene channel is made assuming the  $-\text{NC}$  and  $-\text{CN}$  isomers have similar photoionization cross sections. In considering alternative products, it is conceivable that the CN radical may directly abstract a hydrogen atom from benzene forming HCN and the phenyl radical ( $\text{C}_6\text{H}_5$ ); other indirect pathways could also lead to the elimination of HCN. We checked for these reaction pathways by summing consecutive mass spectra at a photon energy of  $9 \text{ eV}$ . This photon energy is below the AIE of benzene, such that interference from the benzene signal is minimized, but is well above the reported AIE of the phenyl radical ( $8.3\text{--}8.67 \text{ eV}$ , NIST Chemistry Database). No ion signal attributable to phenyl was recorded under these experimental conditions and a limit is established of  $<15\%$  product fraction using a phenyl ionization cross section of  $3 \text{ Mb}$ .<sup>36</sup>

The product detection experiment of CN + toluene reveals only one laser-dependent product for this reaction, observed at  $m/z = 117$  corresponding to  $\text{C}_8\text{H}_7\text{N}$ . The PIE curve corresponding to  $m/z = 117$  is depicted in Figure 6. The most likely species responsible for this signal are the cyanotoluene isomers: ortho, meta, and para. The S/N of the product signal in the CN + toluene experiment was noticeably inferior to the CN + benzene reaction at similar conditions and it was not possible to extract any kinetic information for the product signal. This low product yield may be due to a competitive back-reaction process leading to a regeneration of CN that is suggested by the nonexponential profiles in the room temperature kinetic measurements. This observation is not explored in detail here but it is clear that further studies are required in order to understand the kinetic behavior of the CN + toluene reaction at various temperatures.

The PIE plot depicts the onset of ion signal on the  $m/z = 117$  channel at about  $9.35 \text{ eV}$ . The AIEs of the ortho, meta and para isomers of cyanotoluene are known from photoelectron experiments to be  $9.391 \text{ eV}$ ,  $9.405 \text{ eV}$  and  $9.318 \text{ eV}$ , respectively.<sup>37</sup> The energy resolution of this experiment is  $\sim 40 \text{ meV}$  and, along with the low signal-to-noise of the  $m/z = 117$  signal, it is difficult to distinguish these isomers. Other possible species of the  $\text{C}_8\text{H}_7\text{N}$  formula include bicyclic compounds indole (AIE =  $7.76 \text{ eV}$ ) and indolizine ( $\text{IE}_{\text{vertical}} = 7.24$ ) in addition to the  $-\text{CN}$  and  $-\text{NC}$  conformations of benzyl cyanide. The presence of the bicyclic species can be ruled out on the basis of their low ionization energies. The benzyl cyanide and benzyl isocyanide, although having reported ionization energies close to the onset region measured in Figure 6, are unlikely to be formed from the CN + toluene reaction on mechanistic grounds.

Another plausible reaction pathway for the CN + toluene reaction is the ipso addition channel that has the CN radical binding to the ring carbon of toluene bearing the methyl group. From here, cyanobenzene can be formed from the subsequent elimination of the  $\text{CH}_3$  radical. The ipso addition to toluene

**TABLE 1: Rate Coefficients for the CN + Benzene and CN + Toluene Reactions Obtained with the Laval Nozzle Apparatus**

	$T$ (K)	total flow density ( $10^{16} \text{ cm}^{-3}$ )	aromatic reactant density ( $10^{12} \text{ cm}^{-3}$ )	rate coefficient ( $10^{-11} \text{ cm}^3 \text{ s}^{-1}$ ) <sup>a</sup>
CN + benzene	$105 \pm 5$	2.4	0–50	$43 \pm 9$
	$165 \pm 15$	4.7	0–53	$39 \pm 8$
	$295 \pm 2$	6.7	0–62	$49 \pm 10$
CN + toluene	$105 \pm 5$	2.4	0–50	$13 \pm 3$

<sup>a</sup> Errors in the measured rate coefficient are reported with 20% limits of uncertainty (see text).

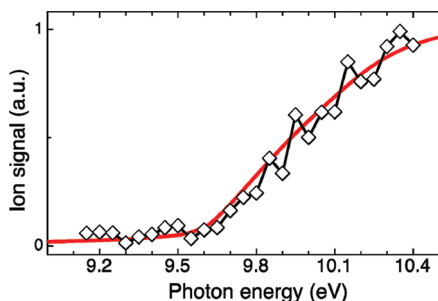


**Figure 5.** Photoionization efficiency (PIE) curve of the  $m/z = 103$  mass channel measured from the room temperature CN + benzene reaction (diamonds) compared to the integrated photoelectron spectrum of cyanobenzene from ref 33.

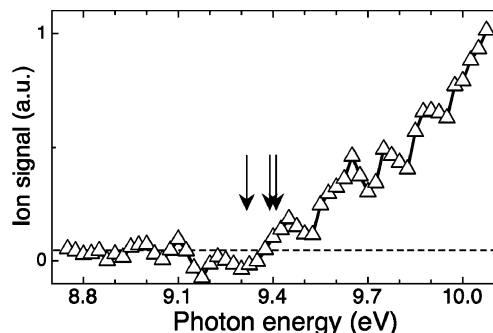


**Figure 6.** Photoionization efficiency (PIE) curve of the  $m/z = 117$  mass channel measured from the room temperature CN + toluene reaction (diamonds). The arrows indicate the adiabatic ionization energies (AIEs) of (from left to right) the para (9.318 eV), ortho (9.391 eV), and meta (9.405 eV) isomers of cyanotoluene (from ref 37).

followed by  $\text{CH}_3$  elimination has been investigated for a range of open-shell species including F, Cl,  $\text{O}(^3\text{P})$ , H, and OH.<sup>38,39</sup> Under the conditions of this experiment we detect no evidence for the formation of cyanobenzene that would indicate a significant ipso elimination channel. Based on the S/N ratio of the experiment and assuming cyanobenzene and cyanotoluene have similar photoionization cross sections we estimate a limit of <15% for the  $\text{CH}_3$  elimination channel.

We also checked for the formation of benzyl radical ( $\text{C}_6\text{H}_5\text{CH}_2$ ) that could be the product of either a direct H-abstraction channel or a complex HCN elimination pathway. The benzyl radical has a known AIE of 7.24 eV.<sup>40,41</sup> Integrating extensively at 8.5 eV photon energy resulted in only a few ion counts on the benzyl radical mass channel. The photoionization cross section of the benzyl radical is not known at this photon energy and we ascribe to the benzyl product channel a limit of <10% based on an estimated ionization cross section of 10 Mb. Overall, under the conditions of these product experiments, the most significant product channel of CN + toluene occurs by radical addition to the ring followed by elimination of a hydrogen atom forming cyanotoluene.

#### 4. Discussion

The apparent lack of temperature response depicted in Figure 4 for the CN + benzene reaction is an indication that the reaction

proceeds without any positive energy barrier along the entrance channel and is also consistent with the formation of an addition complex. Carty et al. have reported similar temperature trends in the rate coefficients for the CN + allene and CN + propyne reactions measured over 15–294 K.<sup>18</sup> The reaction of  $\text{C}_2\text{H} + \text{benzene}$  has also been shown to have a similar large rate coefficient that remains essentially unaffected by temperature over the 105–295 K temperature range.<sup>12</sup> These rate coefficients are very close to the corresponding hard-sphere collision limit, implying reaction efficiencies close to unity.

The measured CN + benzene reaction rates are in good agreement with the recent theoretical predictions of Woon who used quantum chemical calculations with RRKM and master-equation methods to predict bimolecular rates for the CN + benzene reaction over 50–300 K.<sup>31</sup> These data are compared to the experimental data acquired in this current study in Figure 4. The propensity for the  $\text{C}_6\text{H}_6\text{--CN}$  intermediate complex to back-dissociate to the reactants was explored in Woon's study over a range of pressures and temperatures. The computed rates, with zero contribution from back-reaction, were determined to fall within  $(2.8\text{--}3.6) \times 10^{-10} \text{ cm}^3 \text{ molecule}^{-1} \text{ s}^{-1}$  over 50–300 K. The magnitudes of the rate coefficients measured in the current study suggest that back-dissociation of reaction intermediate complexes is negligible under these conditions. It is worth noting that in the same Woon study, rate coefficients for  $\text{C}_2\text{H} + \text{benzene}$  reaction are also reported and compared to experimentally determined values measured previously by our group. The measured rate coefficients are similar to CN + benzene, between  $3 \times 10^{-10}$  and  $4 \times 10^{-10} \text{ cm}^3 \text{ molecule}^{-1} \text{ s}^{-1}$  over 105–295 K, compared to the Woon prediction of  $(2\text{--}3) \times 10^{-10} \text{ cm}^3 \text{ molecule}^{-1} \text{ s}^{-1}$  over the similar temperature range. The computational predictions compare well in both cases, CN + benzene and  $\text{C}_2\text{H} + \text{benzene}$ , but with the computed rate coefficients being systematically less.

A very early kinetic experimental study<sup>19</sup> of various CN + hydrocarbon reactions reported the room temperature rate coefficient for the CN + benzene reaction at  $2.8 \times 10^{-10} \text{ cm}^3 \text{ molecule}^{-1} \text{ s}^{-1}$  compared with the result of  $4.9 \times 10^{-10} \text{ cm}^3 \text{ molecule}^{-1} \text{ s}^{-1}$  reported here. No experimental data for the reaction with benzene appears in that paper so it is difficult to comment on the discrepancy. The authors do mention, however, in the context of a series of CN radical kinetic measurements with various small hydrocarbons, that the results appear in most cases to be close to the gas-kinetic limit and that their CN + benzene result goes against the trend of increased rate with increased hydrocarbon size. That paper also describes the CN + benzene reaction occurring via H-abstraction forming phenyl + HCN. This conclusion is at odds with subsequent studies and the product detection results in this paper that are consistent with an addition–elimination mechanism.

We therefore propose that the reaction of CN + benzene proceeds by radical addition onto any of the benzene carbons, forming an intermediate  $\text{C}_6\text{H}_6\text{--CN}$  radical species. The study of Woon and the combined computational and molecular crossed beam experiments of Balucani et al. both conclude that the

reaction is without barrier and that the radical attack is dominated by the carbon side of the CN radical. Following the CN addition, the  $\text{C}_6\text{H}_6\text{--CN}$  intermediate complex stabilizes by H atom elimination leaving cyanobenzene as the sole coproduct. Computational investigations<sup>22,31</sup> have examined the isocyano ( $\text{--NC}$ ) adduct channel and found that, similar to the  $\text{--CN}$  adduct channel, there is also no positive energy barrier for  $\text{--NC}$  adduct formation. Noteworthy, however, along the  $\text{--NC}$  addition pathway is an initial prereactive complex  $\text{C}_6\text{H}_6\cdots\text{NC}$  situated at  $-17.2\text{ kJ mol}^{-1}$  with respect to the reactants. From here, an  $\sim+6\text{ kJ mol}^{-1}$  barrier separates the prereactive complex from the bound adduct. This intermediate adduct complex ( $\text{C}_6\text{H}_6\text{--NC}$ ) is calculated to be about  $87\text{ kJ mol}^{-1}$  greater in energy than the  $\text{--CN}$  adduct counterpart; i.e. the  $\text{--CN}$  adduct complex sits lower in energy ( $-165.4\text{ kJ mol}^{-1}$ ) than the  $\text{--NC}$  adduct ( $-77.8\text{ kJ mol}^{-1}$ ).<sup>22</sup> Crucially for the  $\text{--NC}$  channel, a  $+29.5\text{ kJ mol}^{-1}$  transition state, relative to the energy of the reactants, separates the  $\text{C}_6\text{H}_6\text{--NC}$  complex and the  $\text{C}_6\text{H}_5\text{NC} + \text{H}$  products. This result suggests that the channel leading to NC products (that is, the formation of isocyanobenzene) would be unfavorable at low temperatures. The rapid rate coefficients measured here vary negligibly over 105–295 K, suggesting that there are no bound prereactive complexes or any significant back-dissociation of intermediate complexes. Stable prereactive complexes, whose formation implies “submerged-reef” barriers, have been identified in systems including  $\text{OH} + \text{isoprene}$ ,<sup>42</sup>  $\text{OH} + \text{ethylene}$ ,<sup>43</sup> and  $\text{CN} + \text{C}_2\text{H}_6$ .<sup>44</sup> These reactions exhibit pronounced negative temperature dependencies down to low temperatures ( $<100\text{ K}$ ). The temperature dependence of the measured rate data appears to rule out any significant presence of a prereactive complex. Product detection studies are not possible in the current Laval nozzle experiment. The room temperature product detection studies of this reaction support the conclusion that the isocyanobenzene product is not formed in any significant quantities and that cyanobenzene + H is the dominant product channel for the CN + benzene reaction.

The 105 K rate coefficient for the CN + toluene reaction is compared to the CN + benzene rate in Figure 4. The measured rate coefficient for CN + toluene is about a factor of 3 less than the CN + benzene reaction. The aforementioned conclusion for CN + benzene is that the reaction is rapid with close to unity reaction efficiencies occurring *via* CN addition channels. For CN + toluene the room temperature product detection results are consistent with CN addition to the CH carbons on the ring of toluene as the main product channel. Although the photoionization data cannot rule out production of benzyl cyanide, this product seems mechanistically unlikely. At the lower temperature of 105 K the barrierless addition of CN onto the phenyl ring of toluene is likely to remain dominant. In order to explain the lower rate coefficient compared to the CN + benzene case, an interaction between CN and the toluene  $\text{--CH}_3$  group needs to be considered. No signal from benzyl radical resulting from a H-abstraction process was recorded in the room temperature product detection studies. At lower temperatures, it is possible that a proportion of CN radicals can interact with the  $\text{--CH}_3$  group of toluene where reaction may be less efficient compared to ring addition. Computational studies exploring the interaction of the CN radical and toluene would be informative particularly with regard to interaction at the terminal methyl group. For the CN +  $\text{C}_2\text{H}_6$  reaction it was shown that a loosely bound van der Waals complex along the H-abstraction channel affected the kinetics down to as low as  $\sim 150\text{ K}$ .<sup>44</sup> In the case of toluene, a dipole–dipole interaction may have a small effect drawing the CN radical to the  $\text{--CH}_3$  group region where a van

der Waals complex could form but a barrier to H-abstraction renders any reaction to be inefficient such that the complex would eventually fall apart. It is also a possibility that a small fraction of back dissociation of the intermediate adduct complexes could contribute to reducing the observed rates. Whether this reduction is due to dissociation from CN adducts at the ipso position or interactions with  $\text{--CH}_3$  remains to be determined. These factors may contribute to the factor of  $\sim 3$  slower rate coefficient at 105 K compared to the CN + benzene case but more studies are required to reveal the dominant cause.

Smith et al. have proposed that, for a radical–neutral reaction, the difference between the ionization energy (IE) of the neutral closed-shell molecule and the electron affinity (EA) of the radical coreactant ( $\text{IE} - \text{EA}$ ) provides predictive insight into the low-temperature reactivity of the reaction pair.<sup>45,46</sup> For  $(\text{IE} - \text{EA}) > 8.75\text{ eV}$  the reaction is likely to encounter a transition state barrier with a positive activation energy (and thus be negligibly slow at low temperatures), but in the case where  $(\text{IE} - \text{EA}) < 8.75\text{ eV}$  this barrier is “submerged” with respect to the energy of the reactants such that the reaction rate is governed by long-range “capture” processes. In this second case the reaction should remain rapid down to low temperatures (20 K). In the two reactions of concern here, the high EA of the CN radical (3.86 eV) and the comparatively low IEs of benzene (9.24 eV) and toluene (8.83 eV) result in  $(\text{IE} - \text{EA}) \ll 8.75\text{ eV}$ . The fast rate coefficients measured in this work at 105 K for both reactions conform to the predictions of Smith et al. that radical–neutral reactions with  $(\text{IE} - \text{EA}) < 8.75\text{ eV}$  will have rates governed by long-range, capture processes. Both reactions are likely to remain rapid down to 20 K.

Generally, CN reactions with unsaturated hydrocarbons that have rate coefficients on the order of  $\sim(3\text{--}4) \times 10^{-10}\text{ cm}^3\text{ molecule}^{-1}\text{ s}^{-1}$  at room temperature tend to have negligible kinetic dependencies on temperature down to 100 K, and this is the case of CN + benzene as shown in this study. The CN + toluene reaction is also rapid at low temperature, but is notably slower than CN + benzene at 105 K. This measurement is the first low temperature rate reported for an alkyl benzene. Computational studies as well as future experimental studies with other radicals, including  $\text{C}_2\text{H} + \text{toluene}$  and  $\text{CH} + \text{toluene}$ , may reveal if the nature of the radical, including the dipole magnitude and orientation, has any affect on the low-temperature reactivity of toluene.

In the context of Titan chemistry, both reactions are rapid at low temperature and therefore are viable under the conditions of Titan’s atmosphere. Whether these reactions could contribute to PANH and haze formation requires further study; there is suggestion of a link between altitude-dependent concentrations of nitriles and haze that would imply a chemical connection.<sup>47</sup> With the significant quantities of benzene detected on Titan, in addition to the presence of many nitrile species including HCN,  $\text{CH}_3\text{CN}$ , and  $\text{C}_2\text{N}_2$  that can photolyze to produce CN,<sup>47</sup> it is plausible that cyanobenzene (mass = 103 Da) is present.

## 5. Conclusion

The findings of this paper are summarized as follows. The CN + benzene reaction has a rapid bimolecular rate coefficient that remains relatively constant over the 105–295 K temperature range. This result suggests that the reaction is without barrier and highly efficient. Using synchrotron-multiplexed photoionization mass spectrometry, the dominant product channel of this reaction at room temperature leads to cyanobenzene + H with no signal attributable to HCN formation, through either HCN elimination or H-abstraction. The CN + toluene bimolecular



rate coefficient has been measured at 105 K. It is also fast but approximately 3 times slower than the CN + benzene reaction at this temperature. This difference may be due to back-dissociation of adduct complexes or interactions with the  $-\text{CH}_3$  group. The room-temperature CN decay profiles measured with toluene displayed a pronounced nonexponential form that suggests back-dissociation of adduct complexes may be significant at this temperature. The synchrotron photoionization measurements reveal that cyanotoluene is the main product channel with no measurable quantities of benzyl ( $\text{C}_7\text{H}_7$ ) from a HCN coproduct channel observed. There are definite implications for Titan chemistry, considering the extensive reports of benzene and nitriles in the atmosphere of this body.

**Acknowledgment.** The support of personnel (A.J.T., F.G.) for this research by the National Aeronautics and Space Administration (grant NAGS-13339) is gratefully acknowledged. Sandia authors and some of the instrumentation for this work are supported by the Division of Chemical Sciences, Geosciences, and Biosciences, the Office of Basic Energy Sciences, the U.S. Department of Energy. Sandia is a multiprogram laboratory operated by Sandia Corp., a Lockheed Martin Co., for the National Nuclear Security Administration under contract DE-AC04-94-AL85000. The Advanced Light Source and Chemical Sciences Division (S.R.L.) are supported by the Director, Office of Science, Office of Basic Energy Sciences of the U.S. Department of Energy under Contract No. DE-AC02-05CH11231 at Lawrence Berkeley National Laboratory.

## References and Notes

- (1) Lavvas, P. P.; Coustenis, A.; Vardavas, I. M. *Planet. Space. Sci.* **2008**, *56*, 27.
- (2) Lavvas, P. P.; Coustenis, A.; Vardavas, I. M. *Planet. Space. Sci.* **2008**, *56*, 67.
- (3) Cui, J.; Yelle, R. V.; Vuitton, V.; Waite, J. H.; Kasprzak, W. T.; Gell, D. A.; Niemann, H. B.; Muller-Wodarg, I. C. F.; Borggren, N.; Fletcher, G. G.; Patrick, E. L.; Raaen, E.; Magee, B. A. *Icarus* **2008**, *200*, 581.
- (4) Waite, J. H.; Niemann, H.; Yelle, R. V.; Kasprzak, W. T.; Cravens, T. E.; Luhmann, J. G.; McNutt, R. L.; Ip, W. H.; Gell, D.; De La Haye, V.; Muller-Wodarg, I.; Magee, B.; Borggren, N.; Ledvina, S.; Fletcher, G.; Walter, E.; Miller, R.; Scherer, S.; Thorpe, R.; Xu, J.; Block, B.; Arnett, K. *Science* **2005**, *308*, 982.
- (5) Waite, J. H.; Young, D. T.; Cravens, T. E.; Coates, A. J.; Crary, F. J.; Magee, B.; Westlake, J. *Science* **2007**, *316*, 870.
- (6) Coustenis, A.; Achterberg, R. K.; Conrath, B. J.; Jennings, D. E.; Marten, A.; Gautier, D.; Nixon, C. A.; Flasar, F. M.; Teanby, N. A.; Bezard, B.; Samuelson, R. E.; Carlson, R. C.; Lellouch, E.; Bjoraker, G. L.; Romani, P. N.; Taylor, F. W.; Irwin, P. G. J.; Fouchet, T.; Hubert, A.; Orton, G. S.; Kunde, V. G.; Vinatier, S.; Mondellini, J.; Abbas, M. M.; Courtin, R. *Icarus* **2007**, *189*, 35.
- (7) Niemann, H. B.; Atreya, S. K.; Bauer, S. J.; Carignan, G. R.; Demick, J. E.; Frost, R. L.; Gautier, D.; Haberman, J. A.; Harpold, D. N.; Hunten, D. M.; Israel, G.; Lunine, J. I.; Kasprzak, W. T.; Owen, T. C.; Paulkovich, M.; Raulin, F.; Raaen, E.; Way, S. H. *Nature* **2005**, *438*, 779.
- (8) Vuitton, V.; Yelle, R. V.; Cui, J. *J. Geophys. Res. Planets* **2008**, *113*.
- (9) Mebel, A. M.; Kislov, V. V.; Kaiser, R. I. *J. Am. Chem. Soc.* **2008**, *130*, 13618.
- (10) Frenklach, M. *Phys. Chem. Chem. Phys.* **2002**, *4*, 2028.
- (11) Smith, I. W. M. *Angew. Chem.* **2006**, *45*, 2842.
- (12) Goulay, F.; Leone, S. R. *J. Phys. Chem. A* **2006**, *110*, 1875.
- (13) Hamon, S.; Le Picard, S. D.; Canosa, A.; Rowe, B. R.; Smith, I. W. M. *J. Chem. Phys.* **2000**, *112*, 4506.
- (14) Hansmann, B.; Abel, B. *ChemPhysChem* **2007**, *8*, 343.
- (15) Goulay, F.; Rebrion-Rowe, C.; Biennier, L.; Le Picard, S. D.; Canosa, A.; Rowe, B. R. *J. Phys. Chem. A* **2006**, *110*, 3132.
- (16) Goulay, F.; Rebrion-Rowe, C.; Le Garrec, J. L.; Le Picard, S. D.; Canosa, A.; Rowe, B. R. *J. Chem. Phys.* **2005**, *122*.
- (17) Sims, I. R.; Queffelec, J. L.; Travers, D.; Rowe, B. R.; Herbert, L. B.; Karthaus, J.; Smith, I. W. M. *Chem. Phys. Lett.* **1993**, *211*, 461.
- (18) Carty, D.; Le Page, V.; Sims, I. R.; Smith, I. W. M. *Chem. Phys. Lett.* **2001**, *344*, 310.
- (19) Bullock, G. E.; Cooper, R. *Trans. Faraday. Soc.* **1971**, *67*, 3258.
- (20) Kaiser, R. I.; Balucani, N. *Acc. Chem. Res.* **2001**, *34*, 699.
- (21) Zhang, F. T.; Kim, S.; Kaiser, R. I.; Jamal, A.; Mebel, A. M. *J. Chem. Phys.* **2009**, *130*.
- (22) Balucani, N.; Asvany, O.; Chang, A. H. H.; Lin, S. H.; Lee, Y. T.; Kaiser, R. I.; Bettinger, H. F.; Schleyer, P. V.; Schaefer, H. F. *J. Chem. Phys.* **1999**, *111*, 7457.
- (23) Trevitt, A. J.; Goulay, F.; Meloni, G.; Osborn, D. L.; Taatjes, C. A.; Leone, S. R. *Int. J. Mass Spectrom.* **2009**, *280*, 113.
- (24) Vakhtin, A. B.; Lee, S.; Heard, D. E.; Smith, I. W. M.; Leone, S. R. *J. Phys. Chem. A* **2001**, *105*, 7889.
- (25) Yaws, C. L.; Narasimhan, P. K.; Gabbula, C. *Yaws' Handbook of Antoine Coefficients for Vapor Pressure*, 2nd electronic ed.; Knovel: New York, 2009.
- (26) Osborn, D. L.; Zou, P.; Johnsen, H.; Hayden, C. C.; Taatjes, C. A.; Knyazev, V. D.; North, S. W.; Peterka, D. S.; Ahmed, M.; Leone, S. R. *Rev. Sci. Instrum.* **2008**, *79*.
- (27) Sims, I. R.; Smith, I. W. M. *Chem. Phys. Lett.* **1988**, *151*, 481.
- (28) Sims, I. R.; Smith, I. W. M. *J. Chem. Soc., Faraday Trans.* **1993**, *89*, 1.
- (29) Russell, J. A.; McLaren, I. A.; Jackson, W. M.; Halpern, J. B. *J. Phys. Chem.* **1987**, *91*, 3248.
- (30) Caballero, J. F.; Jackson, W. M.; Li, X. C.; Sayah, N. *J. Photochem. Photobiol. A—Chem.* **1989**, *47*, 41.
- (31) Woon, D. E. *Chem. Phys.* **2006**, *331*, 67.
- (32) Fally, S.; Carleer, M.; Vandaele, A. C. *J. Quant. Spectrosc. Radiat. Transfer* **2009**, *110*, 766.
- (33) Klasinc, L.; Kovac, B.; Gusten, H. *Pure Appl. Chem.* **1983**, *55*, 289.
- (34) Araki, M.; Sato, S.; Kimura, K. *J. Phys. Chem.* **1996**, *100*, 10542.
- (35) Young, V. Y.; Cheng, K. L. *J. Electron Spectrosc. Relat. Phenom.* **1976**, *9*, 317.
- (36) Sveum, N. E.; Goncher, S. J.; Neumark, D. M. *Phys. Chem. Chem. Phys.* **2006**, *8*, 592.
- (37) Suzuki, K.; Ishiuchi, S.; Sakai, M.; Fujii, M. *J. Electron Spectrosc. Relat. Phenom.* **2005**, *142*, 215.
- (38) Uc, V. H.; Alvarez-Idaboy, J. R.; Galano, A.; Vivier-Bunge, A. *J. Phys. Chem. A* **2008**, *112*, 7608.
- (39) Uc, V. H.; Hernandez-Laguna, A.; Grand, A.; Vivier-Bunge, A. *Phys. Chem. Chem. Phys.* **2002**, *4*, 5730.
- (40) Eiden, G. C.; Weisshaar, J. C. *J. Phys. Chem.* **1991**, *95*, 6194.
- (41) Houle, F. A.; Beauchamp, J. L. *J. Am. Chem. Soc.* **1978**, *100*, 3290.
- (42) Greenwald, E. E.; North, S. W.; Georgievskii, Y.; Klippenstein, S. J. *J. Phys. Chem. A* **2007**, *111*, 5582.
- (43) Greenwald, E. E.; North, S. W.; Georgievskii, Y.; Klippenstein, S. J. *J. Phys. Chem. A* **2005**, *109*, 6031.
- (44) Georgievskii, Y.; Klippenstein, S. J. *J. Phys. Chem. A* **2007**, *111*, 3802.
- (45) Sabbah, H.; Biennier, L.; Sims, I. R.; Georgievskii, Y.; Klippenstein, S. J.; Smith, I. W. M. *Science* **2007**, *317*, 102.
- (46) Smith, I. W. M.; Sage, A. M.; Donahue, N. M.; Herbst, E.; Quan, D. *Faraday Discuss.* **2006**, *133*, 137.
- (47) Bezard, B. *Philos. Trans. R. Soc. A* **2009**, *367*, 683.

JP909633A